Stepwise changes in stratospheric water vapor?

S. Fueglistaler[1]

Received 6 February 2012; revised 21 May 2012; accepted 22 May 2012; published 4 July 2012.

[1] The sparse data available of stratospheric water vapor since the 1950s suggests a positive long-term trend that cannot be explained by the methane increase and what is known about temperature trends around the tropical tropopause, which constrain the amount of water entering the stratosphere. Here, we discuss the 1991–2005 time series of stratospheric water (and methane) measurements from the Halogen Occultation Experiment (HALOE). The high sampling, global coverage and measurement of methane render HALOE data ideal to check the data for self-consistency and to pinpoint the time of changes in entry mixing ratios. In addition to the well-known 'drop' in October 2000, the HALOE data at 10 hPa and less suggest a steep increase in entry mixing ratios shortly before the beginning of the HALOE measurements. Model calculations using simple representations of the stratospheric age of air spectrum in the tropics show that the very dry phase may be explained by a range of scenarios: A long (several years) dry phase followed by a step increase with amplitude 0.3 ppmv; a shorter (≥1 year) dry pulse with amplitude 0.6 ppmv; or steep linear trends over about 2 years with total increases similar to the step scenarios. The drop in October 2000 coincides with anomalously large eddy heat fluxes in the Southern hemisphere and low tropopause temperatures, but no such relation is found for the situation around 1991. The coincidence with the eruption of Mt. Pinatubo is discussed. The evidence for the results presented here is circumstantial, but they would imply that decoupling between stratospheric water trends and tropical tropopause temperatures can occur on short timescales.

Citation: Fueglistaler, S. (2012), Stepwise changes in stratospheric water vapor?, *J. Geophys. Res.*, *117*, D13302, doi:10.1029/2012JD017582.

1. Introduction

[2] Stratospheric water vapor plays an important role for the planetary radiation budget [*Forster and Shine*, 1999], and for stratospheric chemistry. The stratospheric hydrogen budget is dominated by water vapor, methane and hydrogen, and oxidation of methane contributes to stratospheric water vapor. Since molecular hydrogen mixing ratios are observed to be nearly constant in the lower and middle stratosphere [e.g., *Röckmann et al.*, 2003], the complication arising from methane oxidation can be eliminated by considering the sum of water and twice methane mixing ratios, $[HH] = [H_2O] + 2[CH_4]$.

[3] It was early recognized [*Brewer*, 1949] that it is the exceptionally low temperatures at the tropical tropopause that regulate the amount of water entering the stratospheric overworld (terminology of *Hoskins* [1991]) and indeed much of the lowermost stratosphere too. Seasonal [*Mote et al.*, 1996] and interannual [*Randel et al.*, 1998, 2004; *Fueglistaler and Haynes*, 2005; *Randel et al.*, 2006] variability confirms the tight relationship between water entering the stratosphere and temperatures in the vicinity of the tropical tropopause.

[4] In stark contrast, the SPARC Water vapor report [*Kley et al.*, 2000] and *Rosenlof et al.* [2001] noted a positive long-term trend in stratospheric water vapor that exceeds the contributions from increasing methane mixing ratios over the same period, and would correspond to a large positive temperature trend around the tropical tropopause (about +2 to +4 K for the 1960s to the 2000s [see *Fueglistaler and Haynes*, 2005] that is at odds with the arguably little that is known about the temperature trends in this region [see, e.g., *Seidel et al.*, 2011, and references therein].

[5] The HALOE [*Russell et al.*, 1993] version 19 data of stratospheric water vapor show a sharp drop in entry mixing ratios in late 2000 [*Fueglistaler and Haynes*, 2005; *Randel et al.*, 2006]. This drop is also seen in SAGE II version 6.20 [*Thomason et al.*, 2004] measurements of stratospheric water vapor in the tropics [*Fueglistaler and Haynes*, 2005], whereas the NOAA frostpoint (henceforth NOAA FP) measurements over Boulder, Colorado, show a smoother transition to lower values [*Scherer et al.*, 2008]. The NOAA FP measurements over Boulder, Colorado, are the longest available time series, but the high noise level due to sampling only one location at a low sampling rate render this data set not suited for the detection of rapid changes. Therefore, this analysis focuses on the HALOE

[1]Department of Geosciences and AOS, Princeton University, Princeton, New Jersey, USA.

Corresponding author: S. Fueglistaler, Department of Geosciences, Princeton University, Princeton, NJ 08544, USA. (stf@princeton.edu)

0148-0227/12/2012JD017582

data (covering the period June 1991 to November 2005), and results will be discussed in the context of what is known from measurements of the Microwave Limb Sounder (MLS) instrument (like HALOE on board of the Upper Atmosphere Research Satellite), NOAA FP, SAGE II and Atmospheric Trace Molecule Spectroscopy (ATMOS) instruments.

[6] The central argument of the paper is that a simple model for the upward propagation of HH in the tropical lower/mid stratosphere allows to test the self-consistency of measurements of stratospheric water vapor. The approach provides additional evidence for a sharp drop in water entering the stratosphere in October 2000, and suggest a steep increase around the year 1991 of the same magnitude as the drop in 2000. Section 2 summarizes the data used in this study, and presents the rationale for the simple model. Section 3 shows the results, and section 4 discusses the context and implications of these results, specifically also the fact that the steep increase seen in the earliest HALOE measurements coincides with the eruption of Mt. Pinatubo.

2. Data and Methods

2.1. HALOE Measurements of Water Vapor and Methane

[7] We use HALOE measurements of water vapor and methane mixing ratios as reported in the version 19 data. All profiles were screened to eliminate profiles that may be affected by trip angle issues or lockdown angle issues [*Remsberg et al.*, 1996] (list of affected profiles at http://haloe.gats-inc.com/user_docs/index.php). The profiles are binned into monthly mean, zonal mean gridded values with a latitudinal grid spacing of 10° (grid centered at the equator).

[8] HALOE measures extinction at sunrise and sunset conditions, and we have extensively compared results based on separate sunrise and sunset data. We found that mixing ratio estimates based on sunrise or sunset events can differ within a given month on the order of 0.1 ppmv, but no systematic drift of the two separate data sets over time was found. We concluded that the best estimate of the true monthly mean is the average of all available profiles in a given month/latitude bin.

[9] The observations in the tropical lower to mid-stratosphere are best suited for our analysis (see below). Most of the analysis therefore is based on 'tropical mean' data between 25° South and 25° North. For the calculation of this 'tropical' mean, we allow for linear interpolation in time if a given latitude/month bin does not have data, but has data for the preceding *and* following month. To minimize the impact of uneven sampling in latitude, we require at least 4 (out of 5) valid latitude bins for every valid 'tropical monthly mean'. Months not fulfilling this requirement are treated as no data.

[10] The entry mixing ratios of water vapor and HH are estimated based on the HALOE 'tropical mean' data at 86 hPa, which is just a little above the tropical tropopause. In-mixing of stratospherically older air leads to a small [see, e.g., *Volk et al.*, 1996] tail of older air already at this level (i.e. the observations at this level reflect a spectrum rather than pulse of entry mixing ratios), and this contribution may vary a little with time. Hence, the choice here should be considered simply as giving a *fair* estimate of entry mixing ratios.

2.2. SAGE II Aerosol Surface Density Data and Water Vapor

[11] In order to show the impact of the eruption of Mount Pinatubo on stratospheric aerosol, aerosol surface density data from SAGE II are used [*Thomason et al.*, 1997]. The data is binned to the same grid as the HALOE data, and is used only qualitatively. Further, we use the SAGE II version 6.2 water vapor data [*Thomason et al.*, 2004] to provide additional information for specific aspects of the HALOE record.

2.3. Tropospheric Methane

[12] We assume that the methane entry mixing ratios are given by the tropospheric methane mixing ratios in the tropics. The tropical methane mixing ratios are taken from the NOAA Earth System Laboratory (ESRL) methane measurements [*Dlugokencky et al.*, 1995] at Mauna Loa, Hawaii, for the period 1984–2010. This time series is extended in time back to 1970 using the methane mixing ratios measured in Antarctica [*Etheridge et al.*, 1992; *Dlugokencky et al.*, 1994], whereby we adjusted the data from Antarctica with a constant offset to achieve a good match with the tropics for the overlap period 1984–1992. Note that the spatiotemporal variability of methane renders the absolute value of methane entry mixing ratio more complex than our estimate, but due to the long atmospheric lifetime of methane, our estimate can be assumed to be very accurate in terms of variability in entry mixing ratios for the timescale of years and longer.

2.4. Rationale of Method

[13] Molecular hydrogen production and destruction balance fairly well in the lower and middle stratosphere [e.g., *Le Texier et al.*, 1988], such that measurements of water vapor and methane alone allow closure of the lower/mid stratospheric hydrogen budget away from regions where dehydration may play a role - that is, primarily at lower latitudes. The total hydrogen in the two species water vapor and methane is often expressed as HH, where $[HH] \equiv [H_2O] + 2[CH_4]$. The time series of HH anywhere in the stratosphere away from regions of dehydration is simply the time series of HH at entry into the stratosphere convolved with the age spectrum [*Waugh and Hall*, 2002] at the given location. Dynamical changes in the stratosphere affect both the age spectrum and temperatures around the tropical tropopause, which in turn constrain water vapor entry mixing ratios. On the timescale of years and shorter, variations in HH entry mixing ratios are dominated by variations in water vapor.

[14] Variations in the phase propagation of HH entry mixing ratios are indicative of variations in stratospheric transport [see, e.g., *Niwano et al.*, 2003; *Schoeberl et al.*, 2008]. Here, we wish to use the above property to scrutinize the data for self-consistency, at the cost of neglecting variations in the age spectrum. Specifically, we wish to relate variations in HH entry mixing ratios (HH_{entry}) to variations in HH anywhere in the stratosphere based on a time-mean, latitude-pressure dependent age spectrum:

$$[HH](\phi, p, t) = [HH]_{entry}(t) * h(\phi, p, \tau) \quad (1)$$

where ϕ, p, t are latitude, pressure and time, and $h(\phi, p, \tau)$ is the age spectrum, and * denotes the convolution. Further, it is

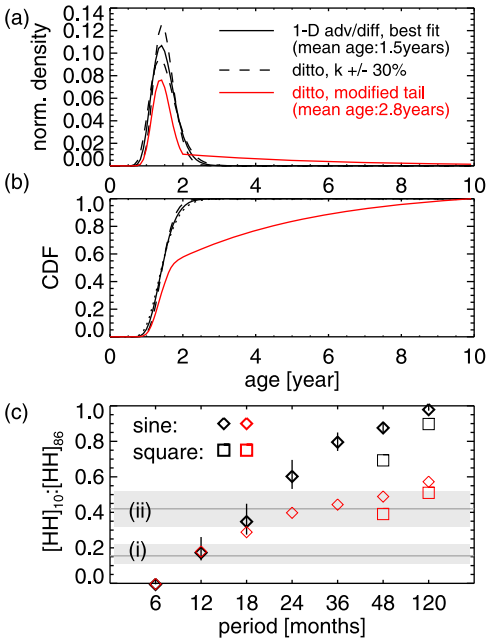

Figure 1. (a) Age of air spectra giving best agreement with observed phase propagation and amplitude attenuation at 10 hPa (see section 3.1). Solutions are not unique; shown are: 1-dimensional advection-diffusion equation (black; sensitivity calculations for variations in diffusivity by ±30%), and (red) the age spectrum with modified tail (exponential with e-folding timescale 5 years). (b) The corresponding cumulative distribution functions. (c) The ratio between input signal amplitude and age-spectrum filtered signal; same color code for age spectra as in Figure 1a. Diamonds: harmonics (ratios determined from least squares fits). Squares: square waveform, ratio determined from half-period means. 'Error bars' for the 1-D advection-diffusion equation show the range of the ratios for a change in diffusivity by ±30% (i.e. the black dashed lines in Figure 1a). The ratios are shown as a function of the period of the input signal, ranging from 6 months to 120 months (10 years). The light grey lines and shaded regions show the slope and error determined from observations from (i) the original data, and (ii) from the ratio of the change in the two sub-period means (before and after 2000); see text and Figure 3.

assumed that there is a single entry mixing ratio for the entire stratosphere. It is known that this is not exactly true [*Rosenlof et al.*, 1997], but for the purpose here air entering the stratosphere is sufficiently mixed in the tropical lower stratosphere to justify this assumption. The above equation can be used to estimate the age spectrum (including its time variations) assuming perfect knowledge of $[\mathrm{HH}](\phi, p, t)$ and $[\mathrm{HH}]_{\mathrm{entry}}(t)$. The approach here is justified if variations in $[\mathrm{HH}](\phi, p, t)$ due to variations in $[\mathrm{HH}]_{\mathrm{entry}}(t)$ are larger than those arising from the time-dependency of the age spectrum (i.e. the age spectrum is also a function of time, $h(\phi, p, t, \tau)$). To leading order, this is indeed the case (see below). As long as the time-dependency does not have a strong trend, neglect of time variations in the age spectrum leads to noise but not a bias in the relation between $[\mathrm{HH}]_{\mathrm{entry}}(t)$ and $[\mathrm{HH}](\phi, p, t)$.

[15] The current understanding of transport and mixing in the stratosphere is that air enters the stratosphere predominantly in the tropics, rises there and subsides at higher latitudes [*Holton et al.*, 1995]. The waves forcing this circulation also lead to mixing, and it is thought that the latitudinal mixing between about 100 hPa and 60 hPa is larger than above, where the tropics (up to about 10 hPa or so) are relatively isolated (the 'tropical pipe' [*Plumb*, 1996] and it's 'leaky' version [*Neu and Plumb*, 1999]; for summary see also *Plumb* [2007]). By averaging over 25°S–25°N we average out much of the variability in $h(\phi, p, t)$ due to the Quasi-Biennial Oscillation (QBO). By focusing on the layer between the tropopause and about 10 hPa we consider a region where the age spectrum is still sufficiently narrow to give variations in $[\mathrm{HH}](\phi, p, t)$ due to variations in $[\mathrm{HH}](t)_{\mathrm{entry}}$ larger than the noise from, for example, low sampling rate. Rewriting equation (1) for the specific region considered here and again assuming no time-dependency of the age spectrum gives

$$[\mathrm{HH}](p,t) = [\mathrm{HH}]_{\mathrm{entry}}(t) * h(p,\tau), \qquad (2)$$

i.e. henceforth we implicitly refer to the region 25°S–25°N unless explicitly stated.

[16] Ideally, the age spectrum should be an analytical function of a few parameters only such that sensitivity of the relation between $[\mathrm{HH}](p, t)$ and $[\mathrm{HH}]_{entry}(t)$ can be explored systematically. The solution to the 1-dimensional advection-diffusion equation [see, e.g., *Waugh and Hall*, 2002] is the simplest solution to this problem (and is indeed frequently used), with the caveat that this solution's tail of old air is less than stratospheric observations indicate. The 'leaky pipe' model by *Neu and Plumb* [1999] gives a better description of reality, at the cost of having more coefficients that need to be empirically determined. We show below that the solution to the 1-dimensional advective-diffusive problem with a somewhat ad-hoc modification to manipulate the tail of the distribution, gives sensible results (limitations discussed).

2.5. The Age Spectrum, and Aspects of Its Time-Filtering Properties

[17] In the absence of sources and sinks for [HH] in the stratosphere, variations therein anywhere in the stratosphere are a phase shifted, low-pass filtered version of $[\mathrm{HH}]_{\mathrm{entry}}(t)$. For example, the correlation of 'tropical' [HH] at 10 hPa with 'tropical' [HH] at 86 hPa gives a phase lag for the maximum correlation of about 17 months, and a slope at this lag of about 0.2; that is, the amplitude of variations at 10 hPa is about 1/5 of that at 86 hPa (numbers taken from results shown in section 3.1).

[18] Figure 1 illustrates the filter behavior of the age spectrum. Figure 1a shows the age spectra at 10 hPa (data shown in section 3.1) of the best fit (with respect to phase lag and amplitude reduction) based on the 1-dimensional advection-diffusion equation (i.e., equation (9) of *Waugh and Hall* [2002]; dotted and dashed lines show age spectra with diffusivity changed by ±30%). The main shortcoming of the solution of the 1-dimensional advection-diffusion equation for the functional form of the age spectrum is the lack of a substantial tail of 'old air'. As a consequence, the age spectrum based on the 1-dimensional advection-diffusion equation reproduces the propagation of the 'tape recorder' signal fairly well, but underestimates the mean age. For 10 hPa, the mean age of the best fit is 1.5 years, much shorter than that

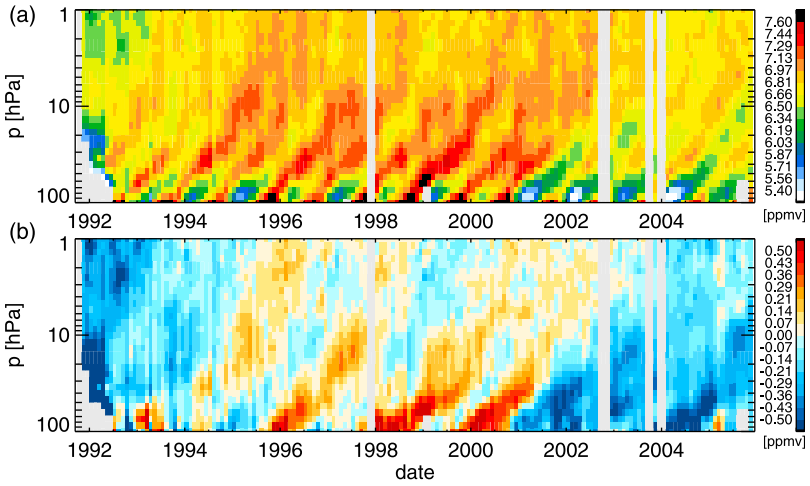

Figure 2. HALOE measurements of (a) HH ([HH] ≡ [H_2O] + 2[CH_4]) and (b) the interannual anomalies HH* after subtracting the mean annual cycle over the period 1994–2005.

reported elsewhere for this region [see, e.g., *Schoeberl et al.*, 2005]. When we replace the tail of the age spectrum with an exponential fall-off, the 'tape recorder' propagation is only little affected, but the mean age increases. For a mean age of 2.8 years (which is more realistic), about 40% is older than 2 years (with an e-folding time of 5 years; results are not sensitive to details of the shape of the tail as long as the mean age is sensible). We will show below that this 'modified' age spectrum also compares better with the [HH] observations presented here. Figure 1b shows the corresponding cumulative distribution frequencies.

[19] Figure 1c shows the slope between variations at the two levels determined by a least squares fit (i.e. the same procedure as applied to the observational data) for harmonic oscillations (circle symbols) for the two age spectra (black and red symbols). The figure shows that the amplitude attenuation varies strongly in the frequency range of interest and that, as expected, the age spectrum with the modified tail attenuates low frequency variations more strongly. The figure also shows (square symbols) results for square waveforms (which would represent stepwise changes) with periods of 4- and 10 years. For these signals, the ratio shown is the ratio of the differences in the means of half periods, between the two levels. The reason for this different approach is because the observational record is limited to only one occurrence of high (1994–2000) and low (2001–2005) values, respectively.

[20] Finally, the two grey areas in Figure 1c (labeled (i) and (ii)) indicate the range (mean plus/minus one standard deviation) of observed ratios, whereby (i) is the linear regression slope of the original data (the average of the slopes determined separately (grey shading shows range from slope +1-std. deviation of higher estimate, to slope −1-std. deviation of lower estimate) for January 1994–October 2000 and November 2000 to November 2005 to remove the effect of the drop in 2000), and (ii) is the ratio of the means for pre-2000 to post-2000 data (i.e. the estimate for the low frequency change; grey shading shows ±1-std. deviation range).

[21] In the following, we will evaluate whether the observations show the theoretically expected frequency dependence of the amplitude decrease as shown in Figure 1.

3. Results

3.1. Overview of HALOE [HH] Measurements

[22] Figure 2a shows the tropical (25°S–25°N, see section 2.1) HALOE [HH] observations, and (panel b) the corresponding interannual anomaly time series [HH]* derived by subtraction of the climatological mean annual cycle evaluated over the period begin of 1994 to end of 2005. The figure shows that the entry mixing ratio variations are dominated by the annual cycle, and propagate upwards - the well-know 'atmospheric tape recorder' [*Mote et al.*, 1996]. The interannual anomalies (Figure 2b) show the same pattern of upward propagation for most of the observational period, with some discontinuities prior to 1994. We will argue below that prior to 1994 measurements may be noisy and biased due to the presence of enhanced stratospheric aerosol, and consequently all 'climatological' variables shown in this paper are based on data from 1994 onwards. The mean phase progression is estimated from the mean annual cycle (results (not shown) are very similar to those presented by *Gregory and West* [2002] and *Hall et al.* [1999]).

3.2. The Frequency Dependence of Amplitude Attenuation With Height

[23] Figure 3 shows, as an example, the scatterplot of the data at 86 hPa versus that at 10 hPa (with appropriate phase lag). In addition to the expected decrease of the amplitude of variations at 10 hPa (the slope is about 1:7), the data points seem to belong to two slightly different groups: those before, and those after the noted drop in the year 2000. There is arguably some subjective judgment in this separation, but note that the separation is based on the theoretical expectation presented above that lower-frequency variations experience less attenuation than higher-frequency variations. The HALOE data shows that (i) the slopes of the linear regressions calculated for each sub-period separately (about 1:7)

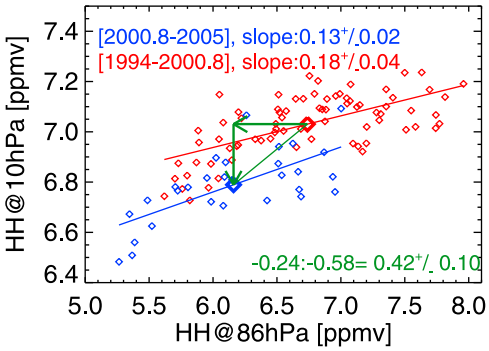

Figure 3. Scatterplot of tropical HALOE HH at 86 hPa and at 10 hPa, with the time series at 10 hPa shifted by the lag with maximum correlation. The red data points refer to the monthly means of the period January 1994 to October 2000 at 86 hPa, and the blue data points to the period November 2000 to November 2005. For each period the results of the linear regression are shown. The bold symbol shows the mean of each period, the green arrow the changes between the periods at each level, together with the ratio of the two changes (given in green). Errors are 1 standard deviation, calculations use standard error propagation.

are identical within their statistical uncertainty; but (ii) the ratio of the changes of the period means (0.42 ± 0.1, or about 1:2.5) is, statistically significantly, much larger. (Results using total least squares instead of ordinary least squares fits are very similar, and only the latter are shown here.) Hence, observations (i) and (ii) are consistent with the hypothesis of a stepwise decrease in 2000, which is a lower frequency change than the variations in each of the sub-periods (by 'lower frequency' we refer here to the fact that the square-signal describing the step from pre- to post-2000 values has a longer period than both the annual cycle and QBO-related variability). Looking back to Figure 1b, the age spectrum tuned for the 12 month variability predicts the observed ratio of 0.42 for the sub-period means for periods (within the error bars) between about 2 and 10 years.

[24] Figure 4 shows the profiles of the correlation coefficients and slopes of the linear regressions of HH*(p)* against HH_{entry} (i.e. here HH(p = 86 hPa) [see also *Gregory and West*, 2002]). Again, the calculations have been done for the full period January 1994 to November 2005 (purple), and for the sub-periods January 1994 to October 2000 (red) and November 2000 to November 2005 (the justification for the pin-pointing of the separation to October 2000 will be shown in section 4). Further, the calculations were done for the original data (solid lines, variability dominated by annual cycle), and for the interannual variability (variability dominated by QBO-related variations with periods of about two years). The correlation coefficient is reasonably high for all calculations except for that of the interannual variability of the period November 2000 to November 2005 when there are fewer data points, and less variability (see Figures 2b and 9a; reasons to be discussed elsewhere).

[25] Overall, the results of the linear regressions are consistent with the expectations: (i) With increasing height, the slope decreases due to mixing. (ii) The slopes of the two sub-periods are identical (within their statistical uncertainty) over most of the altitude range. (iii) The slopes determined from the interannual variability are equal or larger than those for the original data except for the period November 2000 to November 2005. (iv) The slope is largest for the interannual variability of the full period 1994–2006, where the variability is strongly influenced by the drop in October 2000, which corresponds to a square-wave signal with a period of about 10 years or longer (with the observation period 1994 to 2005, only a lower limit for the period can be given).

[26] Hence, this analysis confirms the high quality of the HALOE data and shows that measurements in regions of older stratospheric age provide accurate information about entry mixing ratios a few years earlier. However, the frequency dependency of the filtering of the entry signal limits the possibilities to reconstruct entry mixing ratios based on observations away from the entry region without some knowledge of the frequency of variations in entry mixing ratios.

3.3. A Steep Increase Around the Time of the Pinatubo Eruption?

[27] Figure 5a shows the interannual variability [HH]* just as in Figure 2b, but zoomed in on the first few years of HALOE measurements that we have avoided so far, and extended up to 0.1 hPa. Figure 5b shows [HH]* averaged over the layer 10 hPa − 1 hPa as a function of time and latitude. The figure shows three distinct periods - indicated with the letters 'A', 'B', and 'C'. The physical reality of these periods is supported by the fact that the mixing ratio anomalies propagate at about the mean phase speed determined from the mean annual cycle (the red dots), and the slight delay at higher latitudes seen in Figure 5b. Comparison with Figure 2a shows that periods 'B' and 'C' correspond to the dry/moist periods typical of the measurements up to October 2000. In contrast, period 'A' is as dry (or even slightly drier) than the measurements from November 2000 onwards. Further, the figure shows a very dry patch in the data (indicated by the green arrow) up to about 10 hPa in the first year of the observations.

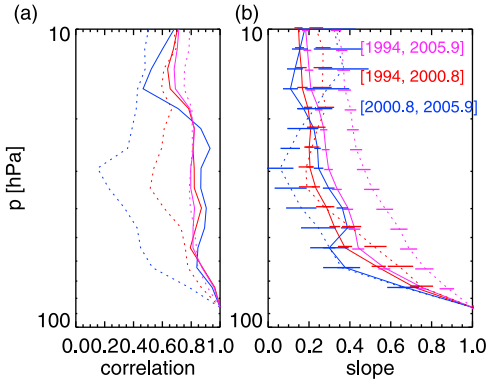

Figure 4. Profiles of the linear regression of HALOE tropical HH time series (shifted with lag of maximum correlation) with that at 86 hPa. (a) The correlation coefficient; (b) the slope of the linear regression. The colors refer to the periods as indicated in figure; the solid line refers to the calculation based on HH; the dotted lines refer to the calculations based on the interannual anomalies [HH]*. Error bars give the 1-sigma uncertainty of the slopes.

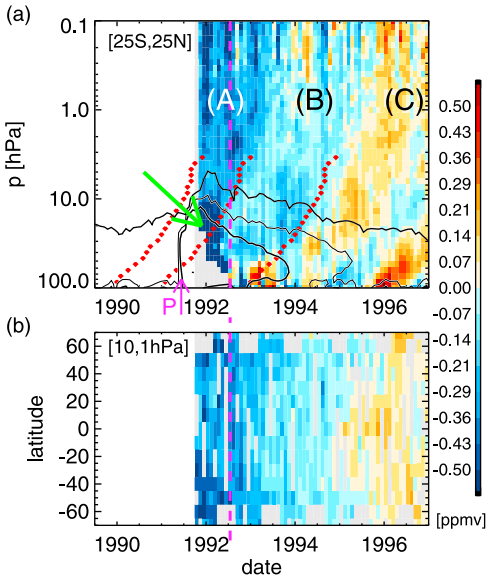

Figure 5. HALOE interannual anomalies HH* (color coded) averaged over (a) the tropics (25°S–25°N, as in other plots), and (b) from 10 hPa – 1 hPa. Data as shown in Figure 2, but for Pinatubo period only, and up to 1 hPa. Also shown in Figure 5a are the time of the eruption of Pinatubo (purple arrow, 'P'), green arrow indicates very low values likely biased by aerosol correction (see text), and aerosol surface density from SAGE II (black contours, thin/thicker/thickest are at 0.5, 2, 8 $\mu m^2 cm^{-3}$). Date (June 1992) of change in procedure of change for locking onto solar disk image shown by dashed purple line. Periods labeled '(A)', '(B)', '(C)' discussed in text.

[28] Figure 5a also shows aerosol surface density measurements from SAGE II (black contour lines). Following the eruption of Mount Pinatubo in June 1991, stratospheric aerosol was massively enhanced. The aerosol increases extinction, and for the water vapor retrieval a correction has to be applied [*Hervig et al.*, 1995]. We suspect that this very dry patch in a region of very high aerosol loading indicates a problem with the aerosol correction (i.e. an overestimate of the extinction due to aerosol). To the best of our knowledge this possible bias has not been discussed in the literature, and we therefore exclude data before 1994 at altitudes below 10 hPa. Also shown is the timing (dashed purple line) of the change of the procedure for locking on the image of the solar disk in June 1992 [see *Remsberg et al.*, 1996], and we observe no correspondence of this date with the variations in HH.

[29] In contrast to the possibly biased measurements below 10 hPa due to the Pinatubo aerosol, the very dry layer (labeled 'A') from 10 hPa upwards shows a plausible phase propagation both with height and latitude. This raises the question whether this dry period was a short period anomaly, or whether the stepwise *decrease* in October 2000 was preceded by a similar steep *increase* in entry mixing ratios around 1991.

3.4. Comparison With MLS/UARS Water Vapor Data

[30] We have argued that the phase propagation of the very dry period 'A' is consistent with atmospheric transport. Here, we show further evidence that the very dry period 'A' is real. The Microwave Limb Sounder (MLS) onboard UARS provides stratospheric water vapor measurements that are in principle unaffected by the Pinatubo aerosol. Unfortunately, these measurements are available only until April 1993 [*Livesey et al.*, 2003], and with only about 1.5 years of data, it is impossible to disentangle interannual variability from the seasonal cycle. MLS has different measurement characteristics (specifically also different vertical resolution), and its reported water vapor variations should not be expected to be exactly identical to those of HALOE. These caveats notwithstanding, Figure 6 shows that the HALOE water vapor and MLS water vapor (both for version 5 [*Livesey et al.*, 2003] and version 6 (referred to as V0104 in publications prior to 2007) data [*Pumphrey*, 1999]) changes in this period are very similar. Comparison of HALOE HH and H_2O shows that air mass displacements lead to some differences between HH and H_2O, but that the contribution to the very low HH values in period 'A' is due to low H_2O and not CH_4. At 10 hPa (which may be still slightly affected by the aerosol, see Figure 5), the dramatic dip in 1992 seen at 1 hPa is less pronounced in the MLS data, and the MLS data of the first few months compared to the last few months is slightly moister (about 0.05 ppmv) than in the HALOE data. Overall, however, the comparison with MLS shows no signs of artifacts in the HALOE data from 10 hPa upwards of that period.

3.5. Forward Model Calculations for Stepwise Changes

[31] The discussed frequency-dependence of attenuation during upward transport (Section 3.2) renders reconstruction of entry mixing ratios from data at 10 hPa during period 'A' impossible (i.e. the inverse problem is underdetermined). Hence, in order to estimate the duration and magnitude of the change in entry mixing ratios we have to resort to forward model calculations. Of course, the forward model calculation does not resolve the under-determination of the problem, but we can constrain the set of possible solutions by requiring that they should have a simple functional form with a small

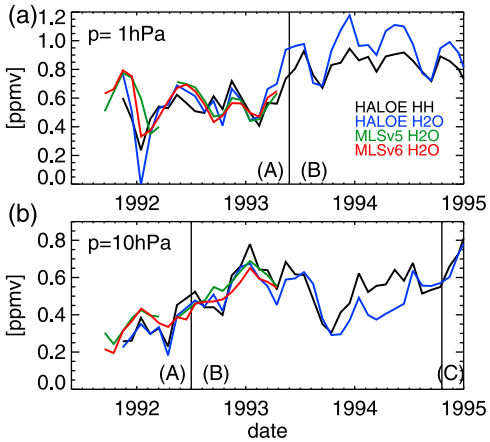

Figure 6. Tropical average (25°S–25°N) monthly mean water vapor (blue) and HH (black) from HALOE, and water vapor from MLS/UARS using version 5 (green) and version 6 (red) data. Absolute values differ, and for each time series a constant offset has been subtracted. Labels '(A)', '(B)' and '(C)' refer to the periods shown in Figure 5, at the approximate times on the 1 and 10 hPa levels.

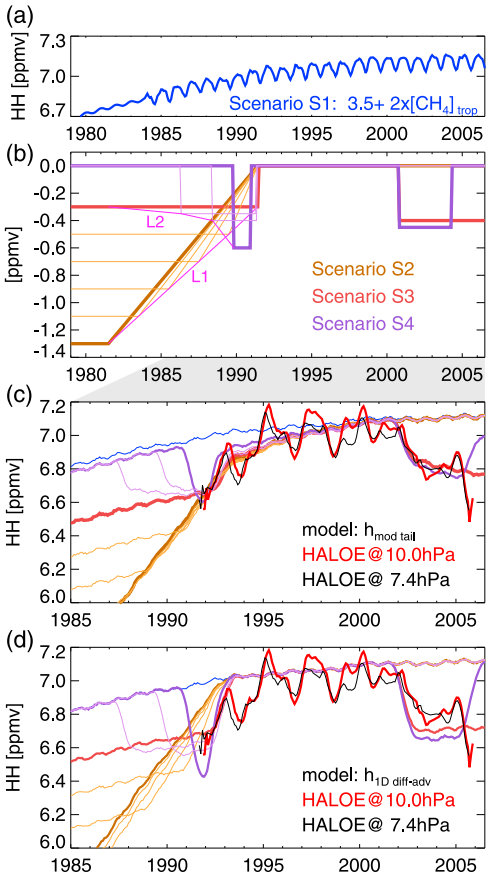

Figure 7. (a) Baseline scenario: constant water vapor entry mixing ratio and tropospheric methane concentrations (see text). (b) Perturbations to S1. Linear trends (solutions bracketed by S2 and S3) and square pulses (solutions bracketed by S3 and S4) that produce agreement with observations at 10 hPa. The magenta lines L1 and L2 indicate the approximate locations of the vertices for equivalent scenarios for 1991. Only square pulses (S3, S4) are considered for 2000. (c) The HALOE observations at 10 hPa (red) and 7.4 hPa (black; shifted to account for phase lag relative to 10 hPa), and the scenarios convolved with the age spectrum for 10 hPa with the modified tail (see text). Note the change in x-axis to focus on HALOE period (indicated by grey shading between panels). (d) Same as Figure 7c, but for age spectrum based on the 1-D advection-diffusion equation (see text).

number of free parameters. We deliberately exclude more or less regular variations due to, for example, the QBO, which is known to be a key factor for interannual variability on timescales of a few years [see, e.g., *Fueglistaler and Haynes*, 2005] through its impact on temperatures around the tropopause. Consequently, the scenarios should be seen as simple representations of the background against which other variations operate. Note that this does not exclude that this 'background' is itself to some extent the result of anomalies in, for example, the amplitude of the QBO-variations, or in the phasing of the QBO and variations in the strength of the stratospheric residual circulation.

[32] In the following, we consider two simple functional forms for the scenarios of entry mixing ratios, whereby we only show solutions that yield sensible agreement with the HALOE data at 10 hPa. The agreement with the HALOE data is only qualitatively determined.

[33] The base scenario (labeled 'S1') assumes that HH entry mixing ratios are the sum of the tropospheric methane mixing ratios ($\times 2$) and a constant water vapor entry mixing ratio tuned such that the average over the period 1995–2000 corresponds to the observed mean HH at 10 hPa over this period. The required mean water entry mixing ratio is 3.5 ppmv, and the scenario is shown in Figure 7a. We then consider the following two perturbations to this base scenario:

[34] 1. A linear trend over a period τ_{trend} with a total change in mixing ratios of Δ (i.e. a slope of Δ/τ_{trend}). This set of scenarios is bounded on one side (labeled 'S2') by the solution for τ_{trend} being much larger than the mean age of air at 10 hPa (in practice, since we truncate the age spectrum at 10 years, this corresponds to $\tau_{trend} = 10$ years). On the other side, the set is bounded by the solution (labeled 'S3') for $\tau_{trend} \rightarrow 0$ (i.e. a step of amplitude Δ).

[35] 2. For the case $\tau_{trend} \rightarrow 0$, we further consider different durations of the perturbation, i.e. the perturbation is a square pulse with duration τ_{step}. Again, the set of solutions is bounded on one side by scenario S3 (which corresponds to $\tau_{step} \rightarrow \infty$), and on the other side is bounded by the shortest τ_{step} that still gives reasonable agreement with data at 10 hPa (this scenario is labeled 'S4', and has $\tau_{step} \sim 1$ year).

[36] For the situation in the year 2000, there is enough HALOE data available before and after the change that we can rule out a slow linear trend. Hence, for this situation we show only the stepwise scenarios (S3 and S4), whereas for the situation in 1991 we show all scenarios.

[37] Figure 7b shows the scenarios that bound the range of possible solutions for both trend (S2, S3) and step scenarios (S3, S4) as bold lines, and some intermediate solutions as thin lines with the corresponding colors (brown for trend, purple for step). Also shown (the magenta line L1) is the approximate position of the vertices for the trend scenarios that have combinations of τ_{trend} and Δ that yield agreement with observations; and the same information for the step scenarios (the magenta line L2). Figure 7c shows the HH mixing ratios at 10 hPa for each scenario based on the convolution with the empirically determined age spectrum for 10 hPa with the modified tail (i.e the previously discussed best fit to the HALOE data), and the HALOE observations at 10 hPa (red) and 7.4 hPa (black). (Recall that the motivation for choosing the 10 hPa level is that this level is low enough such that the tape-recorder signal is still well preserved, and high enough such that the aerosol contamination from Pinatubo is small; the data at 7.4 hPa is shown to give a sense for the uncertainty arising from considering only one specific level.)

[38] Figure 7d shows the same information for the age spectrum based solely on the 1-dimensional advection-diffusion equation. By construction, all scenarios shown agree reasonably with observations for the age spectrum with modified tail (i.e., Figure 7c), and the results for the age spectrum without modified tail are shown only for reference. Figure 7d suggests that it would be possible to find scenarios that more or less agree with observations also for the unmodified age spectrum. However, the far too young mean age of this spectrum renders this set of solutions for water entry mixing ratios less relevant.

[39] From Figure 7 we conclude the following:

[40] 1. The measured variations at 10 hPa and 7.4 hPa are similar, but not identical. The causes of the differences are beyond the scope here. The similarity in the variations suggests that the suspected error arising from the aerosol correction at 10 hPa is smaller than the signal we want to study, but the differences are large enough that only qualitative comparisons can be made. (This is even more true when we consider that the scenarios deliberately do not include QBO variations.)

[41] 2. For the situation in the year 2000, a dry pulse with duration $\tau_{step} \approx 4$ years (with amplitude $\Delta = 0.45$ ppmv) or longer (with amplitude $\Delta = 0.4$ ppmv for $\tau_{step} \rightarrow \infty$) gives reasonable agreement with HALOE data. The range for the duration (about 4 years and longer) determined from the forward model calculation simply confirms what we already knew from the analysis of the filter properties of the age spectrum shown in Figure 1. Extension of the HALOE time series with MLS data on board of Aura, or the NOAA FP data, suggests the most realistic scenario to be similar to scenario S4, but with a positive linear trend instead of a step-like increase at the end of τ_{step}.

[42] 3. For the situation in the year 1991, we find the smallest amplitude required (about 0.3 ppmv) to be for the stepwise increase in 1991 (scenario S3). The scenario with the smallest linear trend (scenario S2) requires a total increase from early 1981 to early 1991 of 1.3 ppmv. The amplitude for the shortest square pulse (scenario S4) is 0.6 ppmv with a duration of one year (shorter pulses with higher amplitudes cannot capture the shape of the observed time series at 10 hPa).

4. Discussion

[43] We have made use of the global sampling at a comparatively high frequency by HALOE to pinpoint the times of changes in water vapor entry mixing ratio. We have argued that combining the information at different pressure levels allows us to test the self-consistency of the data. Our analysis suggests that the period covered by HALOE contains two occurrences of changes in entry mixing ratios that stand out from the average oscillations: In addition to the well-known drop in October 2000 of about -0.4 to -0.5 ppmv, the data suggests also an increase around 1991 of about the same magnitude. The forward model calculations shown in the previous section allow to bracket to some extent the range of water entry mixing ratio variations in this period. The most robust conclusions from these calculations are that entry mixing ratios must have been at least about 0.3 ppmv drier, and that the slope must have been fairly steep, perhaps step-like as in the situation of the year 2000.

[44] These observations raise two questions, addressed below: (i) Are there measurements other than HALOE that can confirm the steep increase around 1991 and the drop in 2000? (ii) What is the relation of these changes in water vapor to the processes controlling conditions around the tropical tropopause?

4.1. Other Measurements

[45] We have shown that the HALOE water vapor above about 10 hPa is consistent with the MLS/UARS observations over the 1.5 years of the MLS/UARS measurements. As with HALOE, the MLS measurements do not provide information about the entry conditions when we suspect a steep increase, and hence cannot further constrain the entry mixing ratios of this period either.

[46] In addition to the measurements by HALOE and MLS onboard of UARS, there exist also measurements from the NOAA FP over Boulder, CO, and global measurements from SAGE II. Further, 4 missions of ATMOS give estimates of water vapor entry mixing ratios for the early/mid 1980's, and the early 1990's.

[47] The ATMOS version 3 data shown by *Michelsen et al.* [2000] show an entry mixing ratio of 3.28 ppmv for the measurements obtained in April/May 1985, 3.53 ppmv for the measurements obtained March/April 1992, 3.67 ppmv for the measurements in April 1993, and 3.65 ppmv for the measurements in November 1994. While it is not possible from these 4 samples to determine whether the changes occur gradually or stepwise, the data does show a general increase from the 1980's to the early 1990's of about 0.3 ppmv.

[48] The NOAA FP measurements over Boulder, CO, show a general increase from the 1980's to the 1990's of a few tenths of a ppmv, and a decrease in the 2000's [see *Scherer et al.*, 2008; *Hurst et al.*, 2011]. While the data is not inconsistent with the hypothesis of changes around 1991 and in October 2000, it cannot be taken as evidence due to noise in the data as a consequence of the low sampling frequency at only one position. An additional problem is the change in instrumentation around 1990 [*Scherer et al.*, 2008], i.e. close to the period when the HALOE data suggests the increase.

[49] Finally, we consider the SAGE II data in some more detail. The global coverage by SAGE II and the fact that the measurements extend back to the 1980's would render this data ideal to test the inferences from the HALOE measurements, in particular also those concerning the very dry period at the beginning of the HALOE measurements. The version 6.2 data [*Thomason et al.*, 2004] is a massive improvement over previous versions, but may still be affected by artifacts that render assessment of the differences to HALOE difficult.

[50] Figure 8 shows the SAGE II data in the tropics (same latitude range, and binning as for HALOE) at 10 hPa (Figure 8a) and at 78 hPa (panel b; levels at higher pressure are more affected by problems with aerosol and clouds). Note that the data at the two levels are plotted on time axes shifted by the approximate phase lag between the two levels. The sparse sampling by SAGE II renders evaluation of a 'tropical mean' difficult, and the figure therefore shows the range of bin-averages, and uses lighter colors for cases where not all bins have valid data. For better comparison of the data at 10 hPa with the data at 78 hPa (where contributions from methane are much smaller), the figure also shows (green data points, anomalies labeled 'SAGE II H_2O*-corr') an estimate of the amount of water at 10 hPa that has entered the stratosphere as water based on the following estimate of the contribution from methane oxidation: The average fraction of oxidized methane at 10 hPa is estimated based on the calculation for scenario S1 and comparison with HALOE methane data for the period 1992–2005. Taking the average fraction captures the overall trends very well, but of course cannot account for the transient fluctuations arising from variations in the age spectrum. The variability of measured water vapor within the tropical band is generally at least as large as the error arising from the simplification in the estimate of the

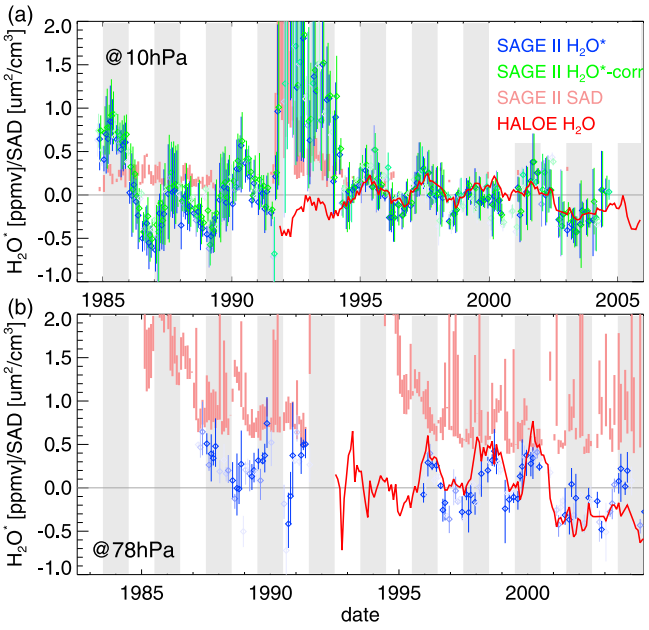

Figure 8. SAGE II version 6.2 water vapor, and surface area density (SAD) measurements in the tropics (between 25°S and 25°N, same bins as for HALOE analysis). (a) Water vapor anomalies at 10 hPa and SAD at 10 hPa. (b) Same as Figure 8a, but for 78 hPa. Note that the time axes are shifted by the approximate phase lag between the two pressure levels. The diamonds show the average over all bins, and the bars give the range of bin averages, with dark colors when data from all bins between 25°S and 25°N is available, and lighter colors for when only a subset of bins is available. The green symbols ('corrected data') show the anomalies at 10 hPa after subtracting the estimated contribution from methane (see text). The red line shows the HALOE tropical average for reference (note for Figure 8b, HALOE data at 73 hPa is shown).

methane contribution, and the latter error is therefore not shown.

[51] The figure shows that SAGE II and HALOE data generally agree reasonably from about 1995 onwards. Due to elevated aerosol levels, no SAGE II water vapor data at 78 hPa are reported before 1987, and between mid-1991 and 1996. At 10 hPa, the water vapor measurements during the Pinatubo period are clearly strongly biased due to the presence of the aerosol. To what extent the slightly elevated aerosol at 10 hPa in the 1980's contributes to the differences in SAGE II water vapor between the 1980's and post-1995 is an open issue. We note that at face value, the SAGE II water vapor mixing ratio from about 1986 to mid-1991 is less (about 0.2 ppmv) than between 1995–2000 (which is qualitatively consistent with the ATMOS and NOAA FP data), and that the amplitudes of the oscillations in the former period are larger. The reasons for the larger oscillations in the 1980's are unclear, and we note that for this period the SAGE II water vapor at lower levels (higher pressure) are not in as good in agreement with those at upper levels as in the post-1995 period.

[52] Taken together, the ATMOS, NOAA FP and SAGE II data cannot strongly constrain the exact shape of the entry mixing ratio curve in the late 1980's/early 1990's either, but they suggest scenarios with very long trends in the 1980's (i.e. scenarios similar to S2) are rather unlikely since the increase from the 1980's to the 1990's measured by these instrument is much smaller than that of these scenarios. Conversely, we can say that the change in water entry mixing ratios in this period must have been steep - i.e. similar to the step-scenario S3 or variants of the square-pulse scenario S4.

4.2. Processes Leading to Stepwise Changes

[53] Stratospheric water vapor entry mixing ratio variations correlate well with zonal mean temperature variations in the vicinity of the tropopause [e.g., *Randel et al.*, 2004]. The distinct spatial pattern of temperatures in this layer [see, e.g., *Fueglistaler et al.*, 2009] implies that zonal mean temperatures cannot be the right metric to estimate entry mixing ratios, however the temporal variability is dominated by zonally symmetric variations, and zonally asymmetric variability (mainly due to ENSO) are of secondary importance [*Fueglistaler and Haynes*, 2005]. Consequently, the zonal mean temperature variations, either at the cold point or on a fixed pressure level, correlate well with water entry mixing ratios.

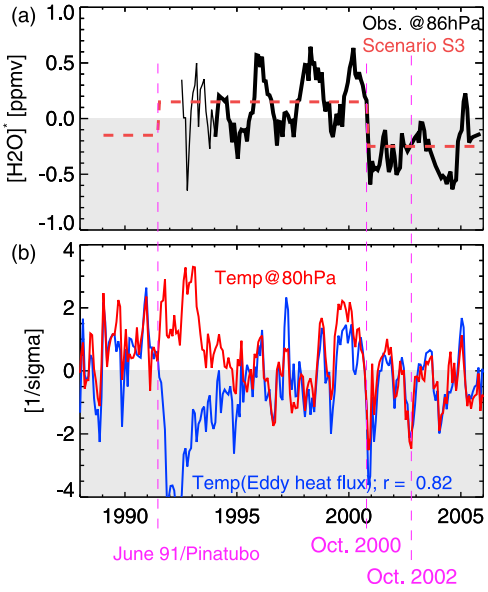

Figure 9. (a) HALOE v19 tropical water vapor anomalies at 86 hPa (black), and scenario S3 for entry mixing ratios. (b) Tropical (35°S–35°N) mean temperatures at 80 hPa (red, in units of standard deviation), and a simple estimate for temperature variability (blue, same units) due to eddy heat flux anomalies [see *Newman et al.*, 2001] based on eddy heat flux at 96 hPa between 20°–70° (both hemispheres) convolved with e-folding timescale of 80 days. Temperature and eddy heat fluxes from ECMWF ERA-Interim data. Anomalies calculated as deviations from mean annual cycle of the period 1995–2005, with the same period used for calculation of the standard deviation (sigma), and the correlation coefficient between the red and blue curves (r = 0.82). Also shown (purple) are the dates of the Pinatubo eruption in June 1991, and two events of anomalous Southern Hemispheric heat fluxes in October 2000 and October 2002.

[54] Correspondingly, the drop in the year 2000 has been linked to a strengthening of the stratospheric residual circulation [*Randel et al.*, 2006]. To produce a step-like change in entry mixing ratios through this mechanism, however, there must also be a step-like increase in the strength of the stratospheric residual circulation.

[55] Figure 9a shows the time series of the tropical HALOE water vapor mixing ratio anomalies at 86 hPa together with scenario S2. Figure 9b shows the European Centre for Medium-range Weather Forecasts (ECMWF) ERA-Interim [*Dee et al.*, 2011] tropical (35°S–35°N) temperature anomalies at 80 hPa (red), which is slightly above the average tropical tropopause. Note that averaging over the tropics eliminates most of the variability due to the QBO, and hence correlation with entry mixing ratios shown in Figure 9a is low. Elimination of much of the QBO variability, however, is necessary to establish a clear picture of the relation to the strength of the residual circulation and trace gas (notably ozone) and aerosol variations.

[56] In addition to temperature, the figure shows an estimate of the temperature variations based on the total eddy heat flux from 6 hourly ERA-Interim wind and temperature at 96 hPa, integrated from 20°–70° on both hemispheres and using a radiative timescale of 80 days. This approach is similar to that used by *Newman et al.* [2001] for the polar vortex, and the figure shows that indeed much of the tropical temperature variability at tropopause levels can be explained by this simple metric (with a correlation coefficient of 0.82 for the period 1995–2005). The figure shows a strong drop in this temperature proxy in October 2000 due to a spike in the Southern hemisphere heat flux. The figure shows that the time of this spike exactly coincides with the drop in observed stratospheric water vapor. A similar spike is observed in October 2002 during the well-documented split of the Antarctic stratospheric vortex. When averaged 5 years before the drop in 2000, and 5 years after, both the temperature as well as the temperature estimate based on the eddy heat flux are slightly lower in the post-2000 period, consistent with the results of *Randel et al.* [2006] showing a stronger residual circulation. However, Figure 9a also shows that the eddy heat flux and tropical average temperatures do not show such a pronounced step in 2000 to a generally lower level as the water vapor does (compare Figure 9b). Also, the relation of eddy heat fluxes before and after the year 2000 depends on the length of the periods considered.

[57] For the period around the eruption of Mt. Pinatubo, the figure shows that the situation is even more complicated. The stratospheric temperature evolution following the eruption of Mt. Pinatubo can be understood as the response to two competing processes: on the one hand, the ECMWF eddy heat flux shows a strongly intensified residual circulation (cooling the tropics), and on the other hand the presence of the aerosol raised the radiative equilibrium temperature (which implies a corresponding warming for fixed radiative heating). Hence, in the situation where the aerosol heating outruns the dynamical effect, one would indeed expect a jump in water entering the stratosphere in mid-1991 (a mechanism discussed in *Joshi and Shine* [2003]). The causality of the enhanced residual circulation is under debate [e.g., *Graf et al.*, 2007], but its effect on temperatures apparently offsets much of the aerosol heating at tropopause levels (which suggests that difficulties explaining the observed temperature variations over the Pinatubo period [*Heckendorn et al.*, 2009] may be rooted not only in the aerosol distribution and aerosol optical properties, but also in the model's dynamical response). The connection of the eruption of Mt. Pinatubo to the water vapor increase from the values of period 'A' to those of period 'B' is also not clear. If the eruption of Mt. Pinatubo did not much change the phase propagation of the water vapor anomalies, Figure 5 suggests that the transition from 'A' to 'B' might have occurred a few months before the eruption.

[58] Independent of the problems with the interpretation of temperatures over the Pinatubo period, HALOE's very low water vapor mixing ratios for air that has entered the stratosphere before the Pinatubo eruption is at odds with ERA-Interim temperatures around the tropical tropopause of that period (red line in Figure 9b, or with temperatures expected from the eddy heat fluxes of that period (blue line in Figure 9b). Comparison of ERA-Interim temperatures with other reanalyses (GMAO/MERRA [*Rienecker et al.*, 2011], and CFSR [*Saha et al.*, 2010]; results to be published separately), and comparison with published temperature data [*Seidel et al.*, 2011, and references therein] shows ERA-Interim temperatures over the relevant period (late 1980's to early 2000's) to be broadly consistent with those of the other data sets. That is, while there may be 'stepwise changes in stratospheric temperature' [*Pawson et al.*, 1998] as a result of a superposition of several processes [*Ramaswamy et al.*, 2006], there is no indication at present that there are steep changes of temperatures around the tropical tropopause that would explain water vapor entry mixing ratios of the pre-Pinatubo period being as low as those after October 2000.

[59] Hence, we conclude that the drop in October 2000 is qualitatively consistent with the temperature evolution, which in turn is qualitatively consistent with a strengthening of the residual circulation. Conversely, the very dry period observed in the earliest HALOE data is difficult to reconcile with what is known about dynamical processes and temperatures at tropical tropopause levels.

[60] Our hypothesis of a steep increase around 1990 is based on circumstantial evidence since HALOE did not measure in this period, and other measurements available over this period do not have the required precision to resolve the question. It is hoped that this work will initiate further analyses of this period to determine whether the decoupling of stratospheric water vapor and tropical tropopause temperature trends occurs on short timescales, and to determine whether the eruption of Pinatubo during this period is causal, or only a coincidence.

[61] **Acknowledgments.** S.F. would like to thank E. Remsberg for information and advice regarding the HALOE data, W. Read for advice on MLS/UARS data, and H. Pumphrey and W. Randel for comments on an early version of this paper. The comments and suggestions from 3 reviewers are greatly appreciated. HALOE data was downloaded from http://haloe.gats-inc.com/home/index.php. MLS/UARS data was downloaded from http://mirador.gsfc.nasa.gov. We thank the NASA Langley Research Center (NASA-LaRC) and the NASA Langley Radiation and Aerosols Branch for providing the SAGE II data, available at http://eosweb.larc.nasa.gov/PRODOCS/sage2/table_sage2.html. We thank NOAA/ESRL for Methane measurements from Mauna Loa, available at http://www.esrl.noaa.gov/gmd/obop/mlo/programs/esrl/methane/methane.html. We thank ECMWF for providing the ERA-Interim data. SF acknowledges support from a NERC Advanced Fellowship during the initial stages of this work.

References

Brewer, A. W. (1949), Evidence for a world circulation provided by the measurements of helium and water vapor distribution in the stratosphere, *Q. J. R. Meteorol. Soc.*, *75*, 351–363.

Dee, D. P., et al. (2011), The ERA-Interim reanalysis: Configuration and performance of the data assimilation system, *Q. J. R. Meteorol. Soc.*, *137*, 553–597.

Dlugokencky, E. J., L. P. Steele, P. M. Lang, and K. A. Masarie (1994), The growth rate and distribution of atmospheric methane, *J. Geophys. Res.*, *99*(D8), 17,021–17,043.

Dlugokencky, E. J., L. P. Steele, P. M. Lang, and K. A. Masarie (1995), Atmospheric methane at Mauna Loa and Barrow observatories: Presentation and analysis of in-situ measurements, *J. Geophys. Res.*, *100*, 23,103–23,113.

Etheridge, D. M., G. I. Pearman, and P. J. Fraser (1992), Changes in tropospheric methane between 1841 and 1978 from a high accumulation-rate Antarctic ice core, *Tellus, Ser. B*, *44*(4), 282–294, doi:10.1034/j.1600-0889.1992.t01-3-00006.x.

Forster, P. M. D. F., and K. P. Shine (1999), Stratospheric water vapour changes as a possible contributor to observed stratospheric cooling, *Geophys. Res. Lett.*, *26*(21), 3309–3312.

Fueglistaler, S., and P. H. Haynes (2005), Control of interannual and longer-term variability of stratospheric water vapor, *J. Geophys. Res.*, *110*, D24108, doi:10.1029/2005JD006019.

Fueglistaler, S., A. E. Dessler, T. J. Dunkerton, I. Folkins, Q. Fu, and P. W. Mote (2009), Tropical tropopause layer, *Rev. Geophys.*, *47*, RG1004, doi:10.1029/2008RG000267.

Graf, H.-F., Q. Li, and M. A. Giorgetta (2007), Volcanic effects on climate: revisiting the mechanisms, *Atmos. Chem. Phys.*, *7*, 4503–4511.

Gregory, A. R., and V. West (2002), The sensitivity of a model's stratospheric tape recorder to the choice of advection scheme, *Q. J. R. Meteorol. Soc.*, *128*, 1827–1845.

Hall, T. M., D. W. Waugh, K. A. Boering, and R. A. Plumb (1999), Evaluation of transport in stratospheric models, *J. Geophys. Res.*, *104*, 18,815–18,839.

Heckendorn, P., D. Weisenstein, S. Fueglistaler, B. P. Luo, E. Rozanov, M. Schraner, L. W. Thomason, and T. Peter (2009), The impact of geoengineering aerosols on stratospheric temperature and ozone, *Environ. Res. Lett.*, *4*, 045108, doi:10.1088/1748-9326/4/4/045108.

Hervig, M. E., J. M. Russell III, L. L. Gordley, J. Daniels, S. R. Drayson, and J. H. Park (1995), Aerosol effects and corrections in the Halogen Occultation Experiment, *J. Geophys. Res.*, *100*(D1), 1067–1079, doi:10.1029/94JD02143.

Holton, J. R., P. H. Haynes, M. E. McIntyre, A. R. Douglass, R. B. Rood, and L. Pfister (1995), Stratosphere-troposphere exchange, *Rev. Geophys.*, *33*, 403–440.

Hoskins, B. J. (1991), Towards a PV-THETA view of the general-circulation, *Tellus, Ser. A*, *43*(4), 27–35, doi:10.1034/j.1600-0870.1991.t01-3-00005.x.

Hurst, D. F., S. J. Oltmans, H. Voemel, K. H. Rosenlof, S. M. Davis, E. A. Ray, E. G. Hall, and A. F. Jordan (2011), Stratospheric water vapor trends over Boulder, Colorado: Analysis of the 30 year Boulder record, *J. Geophys. Res.*, *116*, D02306, doi:10.1029/2010JD015065.

Joshi, M. M., and K. P. Shine (2003), A GCM study of volcanic eruptions as a cause of increased stratospheric water vapor, *J. Clim.*, *16*, 3525–3534.

Kley, D., et al. (2000), SPARC assessment of upper tropospheric and stratospheric water vapour, *WMO/TD No. 1043*, World Meteorol. Org., Geneva, Switzerland.

Le Texier, H., S. Solomon, and R. R. Garcia (1988), The role of molecular hydrogen and methane oxidation in the water vapor budget of the stratosphere, *Q. J. R. Meteorol. Soc.*, *114*, 281–295.

Livesey, N. J., W. G. Read, L. Froidevaux, J. W. Waters, M. L. Santee, H. C. Pumphrey, D. L. Wu, Z. Shippony, and R. F. Jarnot (2003), The UARS Microwave Limb Sounder version 5 data set: Theory, characterization, and validation, *J. Geophys. Res.*, *108*(D13), 4378, doi:10.1029/2002JD002273.

Michelsen, H. A., F. W. Irion, G. L. Manney, G. C. Toon, and M. R. Gunson (2000), Features and trends in Atmospheric Trace Molecule Spectroscopy (ATMOS) version 3 stratospheric water vapor and methane measurements, *J. Geophys. Res.*, *105*, 22,713–22,724.

Mote, P. W., K. H. Rosenlof, M. E. McIntyre, E. S. Carr, J. C. Gille, J. R. Holton, J. S. Kinnersley, and H. C. Pumphrey (1996), An atmospheric tape recorder: The imprint of tropical tropopause temperatures on stratospheric water vapor, *J. Geophys. Res.*, *101*, 3989–4006.

Neu, J. L., and R. A. Plumb (1999), Age of air in a "leaky pipe" model of stratospheric transport, *J. Geophys. Res.*, *104*(D16), 19,243–19,255.

Newman, P. A., E. R. Nash, and J. E. Rosenfield (2001), What controls the temperature of the Arctic stratosphere during the spring?, *J. Geophys. Res.*, *106*(D17), 19,999–20,010.

Niwano, M., K. Yamazaki, and M. Shiotani (2003), Seasonal and QBO variations of ascent rate in the tropical lower stratosphere as inferred from UARS HALOE trace gas data, *J. Geophys. Res.*, *108*(D24), 4794, doi:10.1029/2003JD003871.

Pawson, S., K. Labitzke, and S. Leder (1998), Stepwise changes in stratospheric temperature, *Geophys. Res. Lett.*, *25*(12), 2157–2160.

Plumb, R. A. (1996), A 'tropical pipe' model of stratospheric transport, *J. Geophys. Res.*, *101*(D2), 3957–3972.

Plumb, R. A. (2007), Tracer interrelationships in the stratosphere, *Rev. Geophys.*, *45*, RG4005, doi:10.1029/2005RG000179.

Pumphrey, H. C. (1999), Validation of a new prototype water vapor retrieval for UARS MLS, *J. Geophys. Res.*, *104*(D8), 9399–9412.

Ramaswamy, V., M. D. Schwarzkopf, W. J. Randel, B. D. Santer, B. J. Soden, and G. L. Stenchikov (2006), Anthropogenic and natural Influences in the evolution of lower stratospheric cooling, *Science*, *311*, 1138–1141.

Randel, W. J., F. Wu, J. M. Russell III, A. Roche, and J. W. Waters (1998), Seasonal cycles and QBO variations in stratospheric CH_4 and H_2O observed in *UARS* HALOE data, *J. Atmos. Sci.*, *55*, 163–185.

Randel, W. J., F. Wu, S. J. Oltmans, K. Rosenlof, and G. E. Nedoluha (2004), Interannual changes of stratospheric water vapor and correlations with tropical tropopause temperatures, *J. Atmos. Sci.*, *61*, 2133–2148.

Randel, W. J., et al. (2006), Decreases in stratospheric water vapor since 2001: Links to changes in the tropical tropopause and the Brewer-Dobson circulation, *J. Geophys. Res.*, *111*, D12312, doi:10.1029/2005JD006744.

Remsberg, E. E., P. P. Bhatt, and J. M. Russell III (1996), Estimates of the water vapor budget of the stratosphere from UARS HALOE data, *J. Geophys. Res.*, *101*(D03), 6749–6766.

Rienecker, M., et al. (2011), MERRA: NASA's Modern-Era Retrospective Analysis for Research and Applications, *J. Clim.*, *24*, 3624–3648, doi:10.1175/JCLI-D-11-00015.1.

Röckmann, T., T. S. Rhee, and A. Engel (2003), Heavy hydrogen in the stratosphere, *Atmos. Chem. Phys.*, *3*, 2015–2023.

Rosenlof, K. H., A. F. Tuck, K. K. Kelly, J. M. Russell III, and M. P. McCormick (1997), Hemispheric asymmetries in water vapor and inferences about transport in the lower stratosphere, *J. Geophys. Res.*, *102*(D11), 13,213–13,234.

Rosenlof, K. H., et al. (2001), Stratospheric water vapor increases over the past half-century, *Geophys. Res. Lett.*, *28*, 1195–1198.

Russell, J. M., III, A. F. Tuck, L. L. Gordley, J. H. Park, S. R. Drayson, J. E. Harries, R. J. Cicerone, and P. J. Crutzen (1993), The Halogen Occulation Experiment, *J. Geophys. Res.*, *98*, 10,777–10,797.

Saha, S., et al. (2010), The NCEP Climate Forecast System Reanalysis, *Bull. Am. Meteorol. Soc.*, *91*(8), 1015–1057, doi:10.1175/2010BAMS3001.1.

Scherer, M., H. Vömel, S. Fueglistaler, S. J. Oltmans, and J. Staehelin (2008), Trends and variability of midlatitude stratospheric water vapour deduced from the re-evaluated Boulder balloon series and HALOE, *Atmos. Chem. Phys.*, *8*, 1391–1402.

Schoeberl, M. R., A. R. Douglass, B. Polansky, C. Boone, K. A. Walker, and P. Bernath (2005), Estimation of stratospheric age spectrum from chemical tracers, *J. Geophys. Res.*, *110*, D21303, doi:10.1029/2005JD006125.

Schoeberl, M. R., et al. (2008), QBO and annual cycle variations in tropical lower stratosphere trace gases from HALOE and Aura MLS observations, *J. Geophys. Res.*, *113*, D05301, doi:10.1029/2007JD008678.

Seidel, D. J., N. P. Gillett, J. R. Lanzante, K. P. Shine, and P. W. Thorne (2011), Stratospheric temperature trends: Our evolving understanding, *Wiley Interdiscip. Rev. Clim. Change*, *2*(4), 592–616, doi:10.1002/wcc.125.

Thomason, L. W., L. R. Poole, and T. Deshler (1997), A global climatology of stratospheric aerosol surface area density deduced from Stratospheric Aerosol and Gas Experiment II measurements: 1984–1994, *J. Geophys. Res.*, *102*(D7), 8967–8976.

Thomason, L. W., S. P. Burton, N. Iyer, J. M. Zawodny, and J. Anderson (2004), A revised water vapor product for the Stratospheric Aerosol and Gas Experiment (SAGE) II version 6.2 data set, *J. Geophys. Res.*, *109*, D06312, doi:10.1029/2003JD004465.

Volk, C. M., et al. (1996), Quantifying transport between the tropical and mid-latitude lower stratosphere, *Science*, *272*(5269), 1763–1768.

Waugh, D. W., and T. M. Hall (2002), Age of stratospheric air: Theory, observations, and models, *Rev. Geophys.*, *40*(4), 1010, doi:10.1029/2000RG000101.